

## Direct Determination of the Insulin–Insulin Receptor Interface Using Transferred Cross-Saturation Experiments

Takefumi Nakamura,<sup>†,‡,§</sup> Hideo Takahashi,<sup>\*,§</sup> Mitsuo Takahashi,<sup>†</sup> Nobuhisa Shimba,<sup>†,‡,§</sup> Ei-ichiro Suzuki,<sup>†,‡</sup> and Ichio Shimada<sup>\*,§,||</sup>

<sup>†</sup>The Institute of Life Sciences, Ajinomoto Co. Inc., 1-1 Suzuki-cho, Kawasaki-ku, Kawasaki, Kanagawa, Japan, <sup>‡</sup>Japan Biological Informatics Consortium, 2-41-6 Aomi, Koto-ku, Tokyo, Japan, <sup>§</sup>Biomedical Information Research Center, National Institute of Advanced Industrial Science and Technology, 2-41-6 Aomi, Koto-ku, Tokyo, Japan, and <sup>||</sup>The Graduate School of Pharmaceutical Sciences, The University of Tokyo, 7-3-1 Hongo, Bunkyo-ku, Tokyo, Japan

Received March 26, 2009

Insulin initiates metabolic control by binding to the insulin receptor (IR) on target cells. Kinetic and mutational analyses have revealed two binding sites on the insulin molecule and the residues that compose them. However, direct determination of the insulin-IR interface is required to distinguish those residues that contribute to receptor binding from those required for structural stability. Here, we successfully characterized one binding site using the nuclear magnetic resonance (NMR) transferred cross-saturation method, which can directly determine the binding interface of a large protein–protein complex. The results showed that this binding site contained three residues that have not been identified previously by mutational analyses. On the basis of the structure of the contact site, we also identified a molecule that can displace insulin from the IR. In addition, we discuss the mode of interaction between insulin and its receptor relative to the NMR analyses.

### Introduction

Insulin, a hormone composed of a 21-residue A-chain and a 30-residue B-chain, controls carbohydrate, protein, and fat metabolism. Insulin is stored in the pancreas as a zinc-stabilized hexamer and released into the bloodstream as a zinc-free monomer, where it binds to insulin receptors (IRs<sup>α</sup>) on target cells. The IR is composed of two extracellular 135 kDa  $\alpha$ -subunits and two 95 kDa transmembrane  $\beta$ -subunits. Binding of insulin to the  $\alpha$ -subunit causes conformational changes to the receptor and activates the tyrosine kinase domain of the intracellular  $\beta$ -subunits, thereby inducing a cascade of signaling events inside cells.<sup>1</sup>

Mutational analyses<sup>2–4</sup> and photocross-linking experiments,<sup>5–7</sup> as well as insulin variation among species<sup>8</sup> and the Scatchard plot curvilinear profile that results when insulin binds its receptor,<sup>9</sup> indicate that insulin has two distinct binding sites in the IR. One binding site, site 1, includes GlyA1, IleA2, ValA3, GlnA5, ThrA8, TyrA19, AsnA21, ValB12, TyrB16, GluB23, PheB24, PheB25, and TyrB26.<sup>10,11</sup> Interestingly, the crystal structure indicates that IleA2, ValA3, and TyrB16 are buried within the hydrophobic core and that a conformational change may be required for the interaction of insulin with the IR.<sup>12–14</sup> The other site, site 2, is located opposite site 1 and includes SerA12, LeuA13, GluA17, HisB10, GluB13, and LeuB17.<sup>11,15,16</sup>

On the basis of the results above, De Meyts and Schäffer have proposed a model for insulin binding to the IR. First, insulin contacts the IR with site 2. After a conformational change in the receptor, insulin then makes contact with site 1 and forms a cross-link. The former binding mode results in weak binding, while the latter produces strong binding. Once a second insulin molecule accesses the IR via site 2, the first molecule is released, enabling the second to also bind strongly.<sup>15,16</sup>

In general, the residues suggested by site-directed mutagenesis correspond to those in the protein complex. However, because insulin is a small globular protein with a well-ordered hydrophobic core, site-directed mutagenesis would also cause structural distortion. Therefore, structural biological analyses are necessary to distinguish the residues required for stabilizing insulin conformation from those responsible for direct interaction between insulin and its receptor.

Recently, the three-dimensional structure of the IR ectodomain dimer was determined, revealing many features of the ligand–receptor binding mode and providing insight into the structure of the ligand-binding site of the IR. However, the binding sites on the insulin molecule itself remain to be clarified from this X-ray analysis.<sup>17</sup>

The prevalence of diabetes mellitus has underscored the importance of understanding the interaction between insulin and its receptor. Orally available molecular mimics of insulin could potentially substitute for injected insulin in the treatment of diabetes. In one study, thymolphthalein (TP), which mimics the ValB12, PheB24, and TyrB26 residues of site 1, displaced insulin from its receptor and showed a weak agonist activity.<sup>18</sup> However, the weakness of the activity could reflect the molecule's similarity to site 1 only. To make a potent insulin agonist, it is important to also mimic site 2. To achieve

\*To whom correspondence should be addressed. For H.T.: phone, +81-3-3599-8090; fax, +81-3-3599-8099; E-mail: hid.takahashi@aist.go.jp. For I.S.: phone/fax, +81-3-3815-6540; E-mail: shimada@iw-nmr.f.u-tokyo.ac.jp.

<sup>α</sup>Abbreviations: HSQC, heteronuclear single quantum coherence; IR, insulin receptor; IRFc, Fc-insulin receptor chimera; TP, thymolphthalein; TCS, transferred cross-saturation method.

this, it is highly desirable to gain refined conformational information regarding the contact residues composing site 2 based on structural biological analyses.

In this study, we used the transferred cross-saturation (TCS) method, which directly determines the protein–protein interface of large protein complexes,<sup>19</sup> to investigate the interactions within the soluble insulin–IR complex. Because there is no necessity for chemical substitution nor modification of target molecules, TCS method can precisely determine the binding region even in small proteins such as insulin. To develop a small molecule that binds strongly to the IR, direct determination of the interface of insulin to this receptor, especially at site 2, is required. According to the insulin binding model above, site 2 can be detected in the TCS experiments under excess amounts of insulin relative to the IR because most insulin may exist as free molecules and interaction with the weak-binding site 2 could become dominant. Using this method, we successfully identified the contact residues between the soluble insulin and the IR and correlated them with site 2. Furthermore, on the basis of a chemical shift perturbation experiment, the plausible conformational change of insulin caused by binding at site 2 is discussed. Finally, database searches using the pharmacophore features from site 2 revealed a small molecule capable of competing against insulin for IR binding.

## Results and Discussion

**Binding Sites of Insulin to the IR.** Insulin possesses two distinct binding sites for its receptor, and contact residues have been suggested mainly by mutational studies. However, in the case of a small globular protein with a well-ordered hydrophobic core, site-directed mutagenesis could cause structural distortion. Therefore, it is necessary to distinguish the residues responsible for this interaction from those that are important only for structural stability. In this study, using a highly sensitive TCS method<sup>20</sup> that exploits signals from methyl and aromatic protons, we investigated the interface residues of the soluble insulin in the presence of Fc–insulin receptor chimera (IRFc). IRFc, which consists of the insulin receptor ectodomain fused to the Fc region of the IgG heavy chain, is a soluble fusion protein with the same affinity to insulin as the IR.<sup>21</sup> Seventeen of the 50 insulin residues are detectable by this method (Ile, Leu, Val, Phe, and Tyr) and are distributed almost equally throughout the protein.

Two labeled samples, [<sup>2</sup>H, (<sup>1</sup>H, <sup>13</sup>C-methyl), <sup>15</sup>N]- and [(reduced <sup>1</sup>H), <sup>13</sup>C, <sup>15</sup>N]-soluble insulin, were prepared and exposed to IRFc. The binding sites were detected by comparing the peak intensities on heteronuclear single quantum coherence (HSQC) spectra with and without saturations (Figure 1). Parts a and b of Figure 2 represent the signal reduction ratios. LeuA13, LeuB6, LeuB17, as well as ValB18 (methyl-containing residues) (Figure 2a) and TyrA14 (aromatic-containing residue) (Figure 2b), had reduction ratios more than 30% higher than the mean. The affected residues were located within a limited region of the soluble insulin (Figure 2c) and roughly coincident with the known residues which compose site 2. Then we successfully characterized site 2 using the direct determination method. The affected residues, TyrA14, LeuB6, and ValB18, have not been identified previously as constituents of site 2 in the interaction analyses between insulin and the IR. Thus, we assigned these residues as components of the site as this

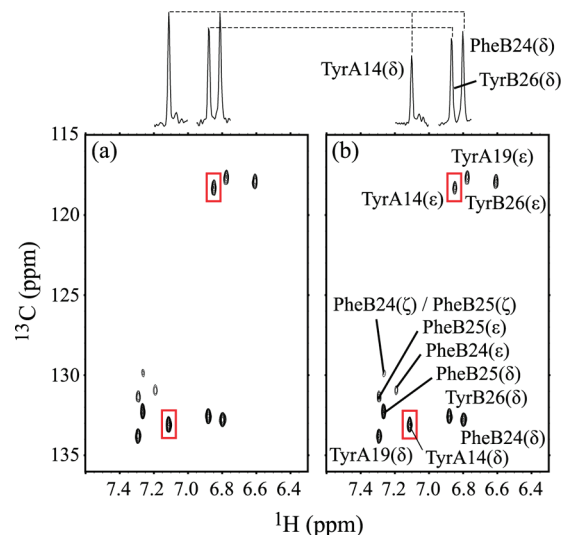


**Figure 1.** The <sup>1</sup>H–<sup>13</sup>C HSQC spectra of [(reduced <sup>1</sup>H), <sup>13</sup>C, <sup>15</sup>N]-soluble insulin (a) without and (b) with irradiation. Red boxes represent the peaks originating from TyrA14. One-dimensional slices above the <sup>1</sup>H–<sup>13</sup>C HSQC spectra clearly indicate that the intensity loss was observed for the resonance originating from TyrA14(δ).

information would be useful for designing a small molecule that binds the IR.

In contrast, no residues in the previously described “classical” site 1 region were detected in our experiments. This could be due to different dissociation rates of the two binding sites. In the complete relaxation and conformational exchange matrix theory,<sup>22</sup> the TCS experiments are applicable to systems with a dissociation rate greater than 0.1 s<sup>-1</sup>. Therefore, we only detected weak binding by site 2 and not the strong binding elicited by both sites 1 and 2. In fact, most of the signals on the <sup>1</sup>H–<sup>15</sup>N HSQC spectrum disappeared when an equal molar ratio of insulin to the IRFc (1:1) was analyzed (data not shown).

### Conformational Change of Insulin upon Binding to the IR.

The chemical shift perturbation experiment was carried out to investigate the effect on insulin of binding to the IRFc. <sup>1</sup>H–<sup>15</sup>N HSQC spectra of the soluble insulin were measured in the absence and presence of IRFc. Because only a small amount of IRFc was added (insulin/IRFc = 15), chemical shift changes at site 2 were not observed. However, chemical shift changes for TyrB26 and GluB27 in the C-terminal region of the B-chain were detected clearly, even in the presence of a small amount of IRFc (Figure 3a). Interestingly, these residues are located opposite site 2 (Figure 3b). The chemical shift change can be caused not only by direct binding but also by a secondary binding effect such as a subtle conformational change induced by binding. Aromatic residues, which can cause large chemical shift changes due to their ring current, are localized at the C-terminal region of the B-chain (PheB24, PheB25, and TyrB26) and could enhance the chemical shift changes of TyrB26 and GluB27.

According to the insulin-receptor binding model by De Meyts and Shäffer, insulin contacts the IR at site 2 and then binds tightly at site 1.<sup>10,15</sup> Conformational changes could occur in the C-terminal region of the B-chain before tight binding at site 1.<sup>12–14</sup> Our NMR results and the B-chain C-terminal region conformational change induced by weak binding with the IRFc reinforce these binding models.

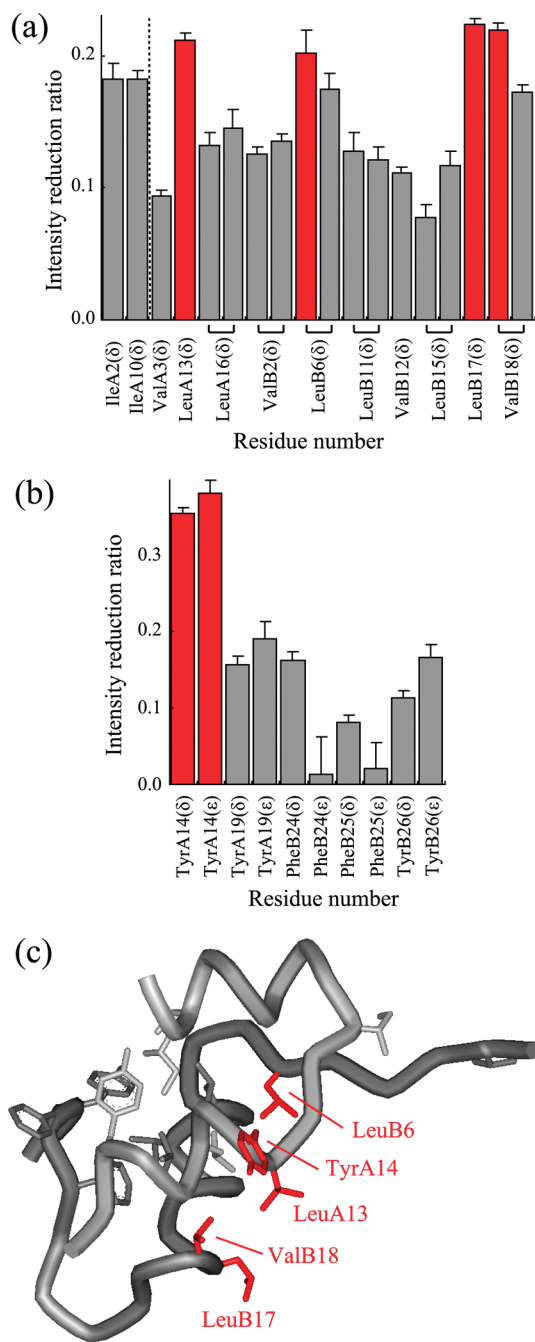


**Figure 2.** Bar graphs of the reduction ratios for the signal intensities with and without irradiation from (a) the methyl-utilizing TCS experiments and (b) the TCS experiments detected by the aromatic resonances. The residues (red) show reduction ratios more than 30% higher than the mean. The standard deviation of the intensity reduction ratio was estimated on the basis of measured background noise levels.<sup>38</sup> Overlapping signals from the prochiral methyl groups of ValA3, LeuA13, ValB12 and LeuB17, and PheB24(ζ) and PheB25(ζ), were excluded from the graphs. (c) Structure of the soluble insulin from the Protein Data Bank (PDB entry 1HUI). The side chains with intensity ratios greater than 30% higher than the mean in the TCS experiments (LeuA13, TyrA14, LeuB6, LeuB17, and ValB18) are shown in red, and the other residues detected in the TCS experiments (Ile, Leu, Val, Phe, and Tyr) are shown in gray.

**Identification of a Small Insulin Mimic.** Using an in-house database, we searched for compounds capable of mimicking the binding site uncovered by the TCS experiments. To select the pharmacophore features, an insulin structure from the

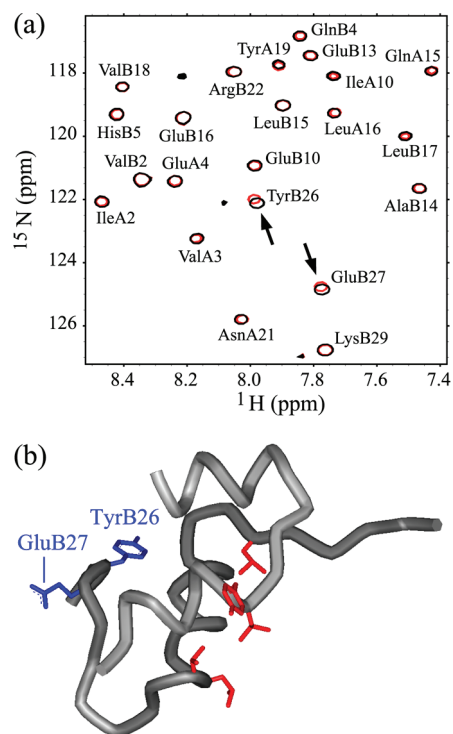


**Figure 3.** (a) An overlay plot of the <sup>1</sup>H-<sup>15</sup>N HSQC spectra of the soluble insulin in the absence (black) and the presence (red) of the IRFc. The resonances originating from TyrB26 and GluB27 are marked with arrows. (b) Structure of the soluble insulin from the Protein Data Bank (PDB entry 1HUI). TyrB26 and GluB27 are shown in blue. These residues are located on the opposite side of site 2 (red).

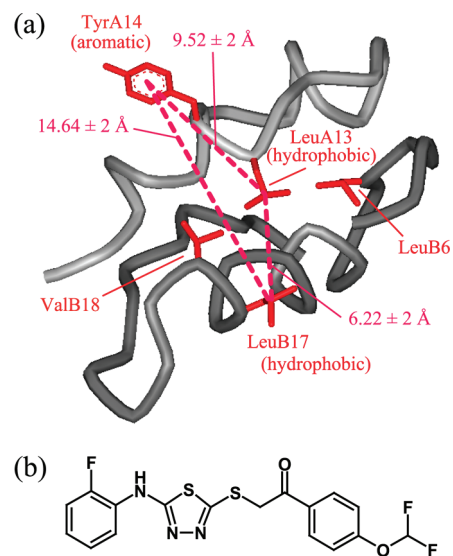


**Figure 4.** (a) Pharmacophore points with the residues of site 2 shown in red. (b) Chemical structure of compound 1, discovered through database searches based on site 2.

Protein Data Bank was used.<sup>23</sup> This insulin mutant retains biological potency and native folding stability, and its high-resolution structures were determined by NMR because it remains monomeric at millimolar concentrations in aqueous solution. We selected three pharmacophore features: the side chain hydrophobic groups in LeuA13 and LeuB17 and an aromatic group in TyrA14 (Figure 4a). Database searches were performed, approximately 500 compounds



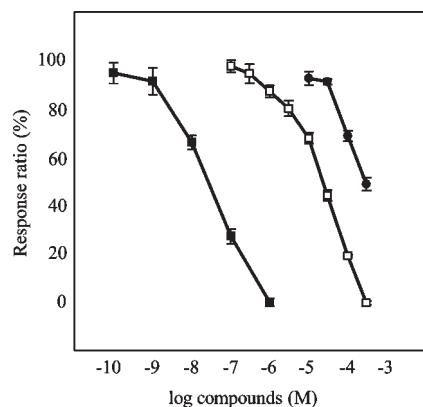


**Figure 5.** Displacement of radioactive insulin from IRFc by (■) native insulin, (□) S371, and (●) compound **1**. All data points are the mean of duplicate samples and shown with standard error bars. Thymolphthalien (TP) showed the enhancement of photons released from the scintillator, and then the binding activity was not estimated properly (data not shown).

were selected, and 59 chemicals were purchased. To confirm our computational findings, the displacement assay was performed using scintillation proximity assays. These studies revealed that 1-[4-(difluoromethoxy)phenyl]-2-({5-[(2-fluorophenyl)amino]-1,3,4-thiazol-2-yl}thio) ethanone (NT23, **1**) (Figure 4b) was able to displace radioactively labeled insulin from the IRFc. The response ratio was 69% at 100  $\mu$ M of compound **1** and 49% at 300  $\mu$ M of compound **1** (Figure 5). Although the displacement activity of compound **1** was weak relative to native insulin and the agonist peptide GSLDES-FYDWFERQLGKK (S371),<sup>24</sup> it showed concentration-dependent binding to the receptor. This result strongly corroborates the contact residues detected by TCS.

It was reported that thymolphthalein (TP), which mimics ValB12, PheB24, and TyrB26 of site 1, displaces insulin from its receptor and shows agonist activity.<sup>18</sup> In contrast, compound **1**, which mimics LeuA13, TyrA14, and LeuB17 of site 2, shows only antagonist activity (data not shown). On the other hand, the phage display experiment identified a series of peptides that bound to two discrete areas of the IR.<sup>24</sup> Some of the peptides were full agonists but of low affinity, while others were either antagonistic or inactive. Interestingly, the peptide that covalently links an agonist peptide with an antagonist peptide, SLEEEWAQVECEVYGRG-CPSGSLDESFYDWFERQLG (S519), showed the strongest agonist activity.<sup>25</sup> Therefore, if compound **1** and TP were connected with linkers of a proper length, a molecule that more closely mimics insulin's interaction with its receptor could be created. In this chimeric compound, the role of the portion of compound **1** may be related to affinity and selectivity toward the IR and that of TP portion might be essential for IR activation.

## Conclusion

Evidence suggests that insulin exhibits two discrete binding sites for its receptor. In this study, we used a sensitive TCS method to clearly define site 2. We identified LeuA13, TyrA14, LeuB6, LeuB17, and ValB18 as the contact residues between the soluble insulin and the IRFc. This binding site contains LeuB6, ValB18, and TyrA14 residues which have not been identified previously within site 2 by mutational analyses. Using pharmacophore points extracted from site 2, a molecule was found that inhibited the interaction between

<sup>125</sup>I-labeled insulin and the IRFc. The interaction of insulin with the IR at both binding sites would be required to activate the tyrosine kinase domain of the intracellular  $\beta$ -subunits and trigger the cascade of signaling events inside the cell. This study further elucidates the interactions between insulin and the IR and may enable the design of novel insulin mimetic agents for the treatment of diabetes mellitus.

## Experimental Section

**Sample Preparation.** Insulin was soluble with mutations in PheB1Glu, HisB10Glu, TyrB16Glu, and ThrB27Glu and a deletion in ThrB30, and the soluble insulin showed 47% biological potency.<sup>26</sup> The soluble insulin was expressed as soluble proinsulin, MEVNQHLCGSELVEALELVCGE;RGFFYEP-KTRREAEDLQVGQVELGGGPGAGSLQPLALEGSLQK-GIVEQCCTSICSLYQLENYCN. The nucleotide fragments encoding the soluble proinsulin were constructed using PCR, subcloned into the pET-22b vector (Novagen, Darmstadt, Germany), and transformed into *Escherichia coli* BL21(DE3) (Novagen). The *E. coli* cells were grown to an  $A_{600}$  of 0.5 at 37 °C, induced with 1 mM IPTG, and incubated for 3 h. Cell pellets were lysed by sonication. The soluble proinsulin in the inclusion body underwent dialysis to enable refolding and disulfide bond formation<sup>27</sup> then purified by a RESOURCE Q column (GE Healthcare UK, Buckinghamshire, England). Appropriate fractions were pooled and the C-chain was cleaved by treatment with a lysyl endopeptidase (Wako, Osaka, Japan). The sample was purified by a COSMOSIL 5-C8-AR-300 column (Nacal Tesque, Kyoto, Japan) (Figure S1 in Supporting Information).

For the chemical shift perturbation experiments, the soluble insulin labeled uniformly with <sup>15</sup>N was prepared by growing cells in minimal media with <sup>15</sup>N-ammonium chloride. The soluble insulin labeled uniformly with <sup>13</sup>C and <sup>15</sup>N for spectral assignments was prepared by growing cells in minimal media with <sup>13</sup>C<sub>6</sub>-glucose (Cambridge Isotope Laboratories, Inc., Cambridge, MA) and <sup>15</sup>N-ammonium chloride (Wako, Osaka, Japan).

For the TCS experiments, selectively methyl-protonated insulin with highly deuterated background<sup>20</sup> was prepared in <sup>2</sup>H<sub>2</sub>O minimal media with [<sup>2</sup>H, <sup>13</sup>C<sub>3</sub>]- $\alpha$ -ketoisovaleric acid (Cambridge Isotope Laboratories, Inc.), [<sup>2</sup>H, <sup>13</sup>C<sub>3</sub>]- $\alpha$ -ketobutyric acid (Cambridge Isotope Laboratories, Inc.), <sup>2</sup>H<sub>7</sub>-glucose (>98% U-<sup>2</sup>H<sub>7</sub>, Cambridge Isotope Laboratories, Inc.), and <sup>15</sup>N-ammonium chloride,<sup>28</sup> yielding [<sup>2</sup>H, (<sup>1</sup>H, <sup>13</sup>C-methyl), <sup>15</sup>N]-soluble insulin. To detect the resonances of aromatic side chains in the TCS experiments, <sup>13</sup>C- and <sup>15</sup>N-labeled and reduced proton-labeled insulin was used and prepared in <sup>2</sup>H<sub>2</sub>O minimal media with <sup>13</sup>C<sub>6</sub>-glucose and <sup>15</sup>N-ammonium chloride,<sup>29</sup> yielding [(reduced <sup>1</sup>H), <sup>13</sup>C, <sup>15</sup>N]-soluble insulin.

An expression vector containing the Fc-insulin receptor chimera (IRFc) was obtained from Dr. T. Izumi (Institute for Molecular and Cellular Regulation, Gunma University, Japan). The IRFc was transiently expressed into FreeStyle 293-F cells (Invitrogen, Carlsbad, CA), which were grown to  $1 \times 10^6$  cells/mL at 37 °C, supplemented with lipid-plasmid complexes, and cultured for 2 d. IRFc in the media was purified by a HiTrap rProtein A FF column (GE Healthcare UK). Specific binding of the soluble insulin and IRFc was confirmed by ELISA. Detailed characterization of IRFc is represented in Figure S2 in Supporting Information.

**NMR Spectroscopy.** All NMR experiments were performed at 37 °C on a Bruker Avance 600 equipped with a cryocooled probe, Avance 700, or Avance 800 spectrometers (Bruker BioSpin GmbH, Karlsruhe, Germany). All spectra were processed by NMRPipe,<sup>30</sup> and data analysis was performed using Sparky.<sup>31</sup>

Sequential assignments of amide group resonances were achieved by three-dimensional triple-resonance experiments, HNCACB and CBCA(CO)NH.<sup>32</sup> All amide group resonances of the main chains were assigned except for the two N-terminal

residues, GlyA1 and GluB1. Assignments of the methyl group resonances were achieved by three-dimensional triple-resonance experiments C(CO)NH and H(CCO)NH.<sup>33</sup> Resonance assignments of the aromatic group were achieved by  $(H_{\beta})C_{\beta}(C_{\gamma}C_{\delta})H_{\delta}$  and  $(H_{\beta})C_{\beta}(C_{\gamma}C_{\delta}C_{\epsilon})H_{\epsilon}$ .<sup>34</sup>

To detect the resonances of insulin in the free state during the TCS experiments, the molar ratio of insulin to the IRFc was 15:1. Methyl-utilizing TCS experiments were performed as follows. [<sup>2</sup>H, (<sup>1</sup>H, <sup>13</sup>C-methyl), <sup>15</sup>N]-soluble insulin and IRFc were dissolved in PBS solution (10 mM phosphate buffer containing 150 mM NaCl), pH 7.2, 99% <sup>2</sup>H<sub>2</sub>O. The final concentration of the soluble insulin was 90 μM and that of the IRFc was 6 μM. Saturation of the IRFc protons was done using the WURST-2 decoupling scheme,<sup>35</sup> followed by <sup>1</sup>H–<sup>13</sup>C CT-HSQC.<sup>36</sup> The irradiation frequency was set at 6.0 ppm, irradiation time was 0.6 s, and the adjusting delay was 1.4 s. For details, see ref 20. To detect the TCS effect using the aromatic resonances, [(reduced <sup>1</sup>H), <sup>13</sup>C, <sup>15</sup>N]-soluble insulin and IRFc were dissolved in PBS solution, pH 7.2, 99% <sup>2</sup>H<sub>2</sub>O. The final concentration of the soluble insulin was 90 μM and that of the IRFc was 6 μM. Saturation of the IRFc protons was done by a series of Gaussian-shaped pulses (50 ms, 1ms delay between pulses,  $\gamma B_1/2\pi = 50$  Hz) for a total irradiation time of 2.5 s, followed by the <sup>1</sup>H–<sup>13</sup>C HMQC detection scheme. Additional delay before the irradiation was 0.5 s. The irradiation frequency was switched from on-resonance (4.7 ppm) for the TCS spectrum to off-resonance (30 ppm) for the reference. As judged by the <sup>1</sup>H–<sup>13</sup>C CT-HSQC experiment,  $\alpha$ -protons of [(reduced <sup>1</sup>H), <sup>13</sup>C, <sup>15</sup>N]-soluble insulin were well deuterated and selective saturation of IRFc was achieved.

In the chemical shift perturbation experiments, the molar ratio of insulin to IRFc was set to 15:1. Samples were dissolved in PBS buffer, pH 6.2, 90% H<sub>2</sub>O/10% <sup>2</sup>H<sub>2</sub>O, and the final concentration of the soluble insulin was 90 μM and that of the IRFc was 6 μM.

**Virtual Screening.** Molecular modeling was performed using the Sybyl program package (Tripos, St. Louis, MO). From the contact residues denoted by the NMR experiments, we selected three pharmacophore features: hydrophobic groups of the side chain in LeuA13 and LeuB17 and an aromatic group in TyrA14. Coordinates for the pharmacophore points were extracted from an insulin Protein Data Bank file, 1HLS.pdb.<sup>23</sup> This mutant structure (TyrB16His mutant insulin, which is in a monomeric state at acidic pH) was used because (1) only a single residue is substituted compared with wild type insulin, and (2) this mutant has the closest structural resemblance to the soluble insulin, which we used in our NMR study.<sup>26</sup> Tolerances (< 2 Å) were applied to the distance between two pharmacophore points to include conformational changes of the protein.

Virtual screenings of commercially available compounds and the in-house database were performed using Unity with the flexible search mode in the Sybyl program package. Drugability of the compounds was assessed by Lipinski's rule-of-five<sup>37</sup> as well as the number of rings (< 5) and rotatable bonds (< 7). Approximately 500 molecules were selected from this search, and 59 chemicals were purchased (Namiki Shoji, Tokyo, Japan; Summit Pharmaceuticals International, Tokyo, Japan).

**Displacement Assay.** The binding activities of chemicals were evaluated using the scintillation proximity assay. The assay buffer contained 20 mM Tris (pH 7.4), 150 mM NaCl, and 0.1% bovine serum albumin without any detergents. The compounds, prepared as 100 mM stock solutions in DMSO, which was used for increasing solubility of chemical compounds, were diluted in assay buffer. DMSO was present at a final concentration of 0.1% (v/v). It is noted that the addition of DMSO and/or the absence of any detergents cause some decrease of the affinity of insulin for IRFc. IRFc was incubated with the compounds, and scintillation proximity beads were precoated with protein A (GE Healthcare UK) in 96-well plates. <sup>125</sup>I-labeled insulin (GE Healthcare UK) was added, and the plates were measured in a topcount plate reader after incubation for 4 h. The response ratio (%) was calculated as  $(C_N - C_S)/(C_N - C_C) \times 100$ , where

$C_N$  represents the photons captured by scintillation counting without unlabeled insulin,  $C_S$  is that with the compounds, and  $C_C$  is that with 1 μM unlabeled insulin.

**Acknowledgment.** This work was supported by grants from the New Energy and Industrial Technology Development Organization. We greatly appreciate the gift of an IRFc expression vector from Prof. T. Izumi (Institute for Molecular and Cellular Regulation, Gunma University, Japan). We wish to thank Dr. N. Fukuchi (Pharmaceutical Research Laboratories, Ajinomoto Co., Inc., Japan) for constructing the scintillation proximity assay system.

**Supporting Information Available:** Purification of the soluble insulin mutant (RP-HPLC chromatogram) and characterization of the IRFc (gel-filtration chromatogram and SDS-PAGE). This material is available free of charge via the Internet at <http://pubs.acs.org>.

## References

- (1) White, M. F.; Kahn, C. R. The insulin signaling system. *J. Biol. Chem.* **1994**, *269*, 1–4, Review.
- (2) Kristensen, C.; Kjeldsen, T.; Wiberg, F. C.; Schäffer, L.; Hach, M.; Havelund, S.; Bass, J.; Steiner, D. F.; Andersen, A. S. Alanine scanning mutagenesis of insulin. *J. Biol. Chem.* **1997**, *272*, 12978–12983.
- (3) Nakagawa, S. H.; Tager, H. S.; Steiner, D. F. Mutational analysis of invariant valine B12 in insulin: implications for receptor binding. *Biochemistry* **2000**, *39*, 15826–15835.
- (4) Xu, B.; Hua, Q.; Nakagawa, S. H.; Jia, W.; Chu, Y.; Katsoyannis, P. G.; Weiss, M. A. Chiral mutagenesis of insulin's hidden receptor-binding surface: structure of an *Allo*-isoleucine<sup>A2</sup> analogue. *J. Mol. Biol.* **2002**, *316*, 435–441.
- (5) Huang, K.; Xu, B.; Hu, S.; Chu, Y.; Hua, Q.; Qu, Y.; Li, B.; Wang, S.; Wang, R.; Nakagawa, S. H.; Theede, A. M.; Whittaker, J.; De Meyts, P.; Katsoyannis, P. G.; Weiss, M. A. How insulin binds: the B-chain  $\alpha$ -helix contacts the L1  $\beta$ -helix of the insulin receptor. *J. Mol. Biol.* **2004**, *341*, 529–550.
- (6) Xu, B.; Hu, S.; Chu, Y.; Wang, S.; Wang, R.; Nakagawa, S. H.; Katsoyannis, P. G.; Weiss, M. A. Diabetes-associated mutations in insulin identify invariant receptor contacts. *Diabetes* **2004**, *53*, 1599–1602.
- (7) Xu, B.; Hu, S.; Chu, Y.; Huang, K.; Nakagawa, S. H.; Whittaker, J.; Katsoyannis, P. G.; Weiss, M. A. Diabetes-associated mutations in insulin: consecutive residues in the B chain contact distinct domains of the insulin receptor. *Biochemistry* **2004**, *43*, 8356–8372.
- (8) Blundell, T. L.; Wood, S. P. Is the evolution of insulin Darwinian or due to selectively neutral mutation? *Nature* **1975**, *257*, 197–203.
- (9) De Meyts, P.; Roth, J.; Neville, D. M., Jr.; Gavin, J. R., III; Lesniak, M. A. Insulin interactions with its receptors: experimental evidence for negative cooperativity. *Biochem. Biophys. Res. Commun.* **1973**, *55*, 154–161.
- (10) De Meyts, P.; Whittaker, J. Structural biology of insulin and IGF1 receptors: implications for drug design. *Nat. Rev. Drug Discovery* **2002**, *1*, 769–783.
- (11) De Meyts, P. The insulin receptor: a prototype for dimeric, allosteric membrane receptors? *Trends Biochem. Sci.* **2008**, *33*, 376–384, Review.
- (12) Derewenda, U.; Derewenda, Z.; Dodson, E. J.; Dodson, G. G.; Bing, X.; Markussen, J. X-ray analysis of the single chain B29-A1 peptide-linked insulin molecule: A completely inactive analogue. *J. Mol. Biol.* **1991**, *220*, 425–433.
- (13) Hua, Q. X.; Shoelson, S. E.; Kochoyan, M.; Weiss, M. A. Receptor binding redefined by a structural switch in a mutant human insulin. *Nature* **1991**, *354*, 238–241.
- (14) Ludvigsen, S.; Olsen, H. B.; Kaarsholm, N. C. A structural switch in a mutant insulin exposes key residues for receptor binding. *J. Mol. Biol.* **1998**, *279*, 1–7.
- (15) De Meyts, P. The structural basis of insulin and insulin-like growth factor-1 receptor binding and negative cooperativity, and its relevance to mitogenic versus metabolic signaling. *Diabetologia* **1994**, *37*, S135–S148.
- (16) Schäffer, L. A model for insulin binding to the insulin receptor. *Eur. J. Biochem.* **1994**, *221*, 1127–1132.
- (17) McKern, N. M.; Lawrence, M. C.; Streltsov, V. A.; Lou, M.; Adams, T. E.; Lovrecz, G. O.; Elleman, T. C.; Richards, K. M.;

- Bentley, J. D.; Pilling, P. A.; Hoyne, P. A.; Cartledge, K. A.; Pham, T. M.; Lewis, J. L.; Sankovich, S. E.; Stoichevska, V.; Da Silva, E.; Robinson, C. P.; Frenkel, M. J.; Sparrow, L. G.; Fernley, R. T.; Candana Epa, V.; Ward, C. W. Structure of the insulin receptor ectodomain reveals a folded-over conformation. *Nature* **2006**, *443*, 218–221.
- (18) Schlein, M.; Ludvigsen, S.; Olsen, H. B.; Andersen, A. S.; Danielsen, G. M.; Kaarsholm, N. C. Properties of small molecules affecting insulin receptor function. *Biochemistry* **2001**, *40*, 13520–13528.
- (19) Nakanishi, T.; Miyazawa, M.; Sakakura, M.; Terasawa, H.; Takahashi, H.; Shimada, I. Determination of the interface of a large protein complex by transferred cross-saturation measurements. *J. Mol. Biol.* **2002**, *318*, 245–249.
- (20) Takahashi, H.; Miyazawa, M.; Ina, Y.; Fukunishi, Y.; Mizukoshi, Y.; Nakamura, H.; Shimada, I. Utilization of methyl proton resonances in cross-saturation measurement for determining the interfaces of large protein–protein complexes. *J. Biomol. NMR* **2006**, *34*, 167–177.
- (21) Bass, J.; Kurose, T.; Pashmforoush, M.; Steiner, D. F. Fusion of insulin receptor ectodomains to immunoglobulin constant domains reproduces high-affinity insulin binding in vitro. *J. Biol. Chem.* **1996**, *271*, 19367–19375.
- (22) Jayalakshmi, V.; Krishna, N. R. Complete relaxation and conformational exchange matrix (CORECEMA) analysis of intermolecular saturation transfer effects in reversibly forming ligand–receptor complexes. *J. Magn. Reson.* **2002**, *155*, 106–118.
- (23) Ludvigsen, S.; Roy, M.; Thøgersen, H.; Kaarsholm, N. C. High-resolution structure of an engineered biologically potent insulin monomer, B16 Tyr → His, as determined by nuclear magnetic resonance spectroscopy. *Biochemistry* **1994**, *33*, 7998–8006.
- (24) Pillutla, R. C.; Hsiao, K.; Beasley, J. R.; Brandt, J.; Ostergaard, S.; Hertz Hansen, P.; Spetzler, J. C.; Danielsen, G. M.; Andersen, A. S.; Brissette, R. E.; Lennick, M.; Fletcher, P. W.; Blume, A. J.; Schäffer, L.; Goldstein, N. I. Peptides identify the critical hotspots involved in the biological activation of the insulin receptor. *J. Biol. Chem.* **2002**, *277*, 22590–22594.
- (25) Schäffer, L.; Brissette, R. E.; Spetzler, J. C.; Pillutla, R. C.; Ostergaard, S.; Lennick, M.; Brandt, J.; Fletcher, P. W.; Danielsen, G. M.; Hsiao, K.; Andersen, A. S.; Dedova, O.; Ribet, U.; Hoeg-Jensen, T.; Hertz Hansen, P.; Blume, A. J.; Markussen, J.; Goldstein, N. I. Assembly of high-affinity insulin receptor agonists and antagonists from peptide building blocks. *Proc. Natl. Acad. Sci. U. S. A.* **2003**, *100*, 4435–4439.
- (26) Olsen, H. B.; Ludvigsen, S.; Kaarsholm, N. C. Solution structure of an engineered insulin monomer at neutral pH. *Biochemistry* **1996**, *35*, 8836–8845.
- (27) Mackin, R. B. Streamlined procedure for the production of normal and altered versions of recombinant human proinsulin. *Protein Expression Purif.* **1999**, *15*, 308–313.
- (28) Goto, N. K.; Gardner, K. H.; Mueller, G. A.; Willis, R. C.; Kay, L. E. A robust and cost-effective method for the production of Val, Leu, Ile ( $\delta$ 1) methyl-protonated  $^{15}\text{N}$ -,  $^{13}\text{C}$ -,  $^2\text{H}$ -labeled proteins. *J. Biomol. NMR* **1999**, *13*, 369–374.
- (29) Shekhtman, A.; Ghose, R.; Goger, M.; Cowburn, D. NMR structure determination and investigation using a reduced proton (REDPRO) labeling strategy for proteins. *FEBS Lett.* **2002**, *524*, 177–182.
- (30) Delaglio, F.; Grzesiek, S.; Vuister, G. W.; Zhu, G.; Pfeifer, J.; Bax, A. NMRPipe: a multidimensional spectral processing system based on UNIX pipes. *J. Biomol. NMR* **1995**, *6*, 277–293.
- (31) Goddard, T. D.; Kneller, D. G. *SPARKY3*; University of California, San Francisco.
- (32) Clore, G. M.; Gronenborn, A. M. Multidimensional heteronuclear nuclear magnetic resonance of proteins. *Methods Enzymol.* **1994**, *239*, 349–363.
- (33) Grzesiek, S.; Anglister, J.; Bax, A. Correlation of backbone amide and aliphatic side-chain resonances in  $^{13}\text{C}/^{15}\text{N}$ -enriched proteins by isotropic mixing of  $^{13}\text{C}$  magnetization. *J. Magn. Reson., Ser. B* **1993**, *101*, 114–119.
- (34) Yamazaki, T.; Forman-Kay, J. D.; Kay, L. E. Two-dimensional NMR experiments for correlating  $^{13}\text{C}\beta$  and  $^1\text{H}\delta/\epsilon$  chemical shifts of aromatic residues in  $^{13}\text{C}$ -labeled proteins via scalar couplings. *J. Am. Chem. Soc.* **1993**, *115*, 11054–11055.
- (35) Takahashi, H.; Nakanishi, T.; Kami, K.; Arata, Y.; Shimada, I. A novel NMR method for determining the interfaces of large protein–protein complexes. *Nat. Struct. Biol.* **2000**, *7*, 220–223.
- (36) Vuister, G. W.; Bax, A. Measurement of two-bond  $J_{\text{COH}\alpha}$  coupling constants in proteins uniformly enriched with  $^{13}\text{C}$ . *J. Biomol. NMR* **1992**, *2*, 401–405.
- (37) Lipinski, C. A. Drug-like properties and the causes of poor solubility and poor permeability. *J. Pharmacol. Toxicol. Methods* **2000**, *44*, 235–249, Review.
- (38) Farrow, N. A.; Muhandiram, R.; Singer, A. U.; Pascal, S. M.; Kay, C. M.; Gish, G.; Shoelson, S. E.; Pawson, T.; Forman-Kay, J. D.; Kay, L. E. Backbone dynamics of a free and phosphopeptide-complexed Src homology 2 domain studied by  $^{15}\text{N}$  NMR relaxation. *Biochemistry* **1994**, *33*, 5984–6003.